

# Synthesis and Electrogenerated Chemiluminescence of PbS Nanospheres

Jun Geng<sup>1,2</sup>, Bo Liu<sup>1</sup>, Guifen Jie<sup>1</sup>, and Jun-Jie Zhu<sup>1,\*</sup>

<sup>1</sup>Key Laboratory of Analytical Chemistry for Life Science (MOE), School of Chemistry and Chemical Engineering, Nanjing University, Nanjing 210093, P. R. China

<sup>2</sup>Department of Chemistry, Jiangsu Institute of Education, Nanjing 210013, P. R. China

The uniform PbS nanospheres with an average diameter of 110 nm were synthesized via a sonochemical approach using PVP as a template reagent in aqueous solution. The chemiluminescence of the as-prepared PbS induced by electrochemical method was investigated. Stable electrogenerated chemiluminescence was first observed from the PbS nanospheres in the existence of peroxodisulfate ions.

**Keywords:** PbS, Sonochemistry, Electrogenerated Chemiluminescence, Nanosphere.

## 1. INTRODUCTION

The II–VI semiconductor nanoparticles have outstanding electronic and optical properties and are useful in novel nanodevices such as light-emitting diodes,<sup>1</sup> single-electron transistors,<sup>2</sup> and field-effect thin-film transistors.<sup>3</sup> Among the II–VI semiconductors, lead sulfide (PbS) is unique for having the near-infrared band gap of 0.41 eV in the bulk form and a large exciton Bohr radius of 18 nm.<sup>4</sup> Its band gap can be widened to the visible region of about 2 eV by forming nanoclusters.<sup>5</sup> Consequently, PbS nanocrystals are potentially useful in electroluminescent devices and optical devices. Because of that, much effort has been devoted to the development of synthetic methods for PbS particles with various controllable sizes and shapes. A lot of routes, including microwave irradiation, solid-state reaction, photochemical reaction, electrochemical method,<sup>6–9</sup> have been reported. In this paper, PbS nanospheres were synthesized via an one-stage sonochemical method using PVP as a template reagent in aqueous solution. The as-prepared product is nanospheres with size of ~110 nm in diameter. Further investigations are concentrated on the electrogenerated chemiluminescence (ECL) of the PbS nanospheres.

ECL has been extensively used to investigate the nature of an emitting state, the mechanism by which it is produced, and electron transfer. As a rule to generate ECL, the electrogenerated reduced and oxidized species have to be stable enough to be able to form excited state complexes. Use of coreactants such as persulfate and oxalate is useful

especially when one of  $R^+$  or  $R^-$  is not stable enough for ECL reaction, or when the ECL solvent has a narrow potential window so that  $R^+$  or  $R^-$  cannot be formed. It has been reported that some semiconductor nanomaterials such as Si,<sup>10</sup> Ge,<sup>11</sup> CdS,<sup>12</sup> CdSe,<sup>13</sup> CdTe<sup>14</sup> and ZnO<sup>15</sup> can generate luminescence when going through an electrochemistry process. Furthermore, the ECL behavior of semiconductor nanocrystals was found to be dependent and more sensitive to the particle surface states as compared to the bulk counterpart. Here ECL from dispersed PbS nanospheres in alkali solution are observed for the first time. We have also discussed the stability of both oxidized and reduced forms that were electrogenerated when the electrode potential was cycled between positive and negative values.

## 2. EXPERIMENTAL DETAILS

### 2.1. Materials

All the reagents used were of analytical purity and were used without further purification. Lead (II) acetate ( $Pb(CH_3COO)_2 \cdot 3H_2O$ ), PVP-K30, thioacetamide (TAA) were purchased from Beijing Chemical Reagents Ltd. Co. of China. Absolute ethanol was purchased from Shanghai Second Chemical Reagent Factory of China.

### 2.2. Synthesis

$Pb(CH_3COO)_2 \cdot 3H_2O$  (3.79 g, 0.01 mol) and PVP-K30 (1.0 g) were dissolved in 100 mL distilled water.

\*Author to whom correspondence should be addressed.

Afterwards, TAA (0.75 g, 0.01 mol) was added to the above mixture and the solution was irradiated with a high-intensity ultrasonic irradiation (Sonic, 20 KHz, 75 W/cm<sup>2</sup>) under ambient conditions. Following a 30 min ultrasonication step, a black precipitate was obtained. The precipitate was centrifuged and washed with distilled water and absolute ethanol in sequence, and then air-dried for the succeeding experimental measurements.

### 2.3. Characterization

The XRD analysis was performed by a Philips X'pert X-ray diffractometer at a scanning rate of 4°/min in the 2 $\theta$  range from 10° to 80°, with graphite monochromatized Cu K $\alpha$  radiation ( $\lambda = 0.15418$  nm). TEM patterns were recorded on a JEOLJEM 200CX transmission electron microscope, using an accelerating voltage of 200 kV. SEM images were taken on a JEOL JSM-6360LV scanning electron microscope. The UV-Vis absorption spectra were measured on a Ruili 1200 spectrophotometer (Peking Analytical Instrument Co.) Cyclic voltammograms (CVs) and ECL curves were recorded simultaneously on a MPI-A Electrochemiluminescence Analyzer (Xi'An Remax Electronic Science & Technology Co. Ltd. Xi'An, China) with a photomultiplier tube (PMT) held at 800 V.

An electrochemical cell consisted of a carbon-pasted working electrode, a Pt wire counter electrode, and an Ag/AgCl reference electrode. The carbon-paste electrode was fabricated by mixing graphite powder and the as-prepared PbS nanospheres (6:1 mass ratio) in ethanol. After drying, a homogenized graphite/PbS mixture was achieved. Subsequently, paraffin oil was added into the mixture (oil:mixture = 1:4 mass ratio) and thoroughly mixed until a homogeneous paste was obtained. The prepared paste was packed into a glass tube with a 4 mm inner diameter and electrical contact was established with a copper rod through the back of the electrode. Afterwards, the electrode surface was polished with smooth paper.

## 3. RESULTS AND DISCUSSION

### 3.1. Characterization of the Final Products

Figure 1 shows the XRD pattern of the as-prepared products. The diffraction peaks of the products can be all indexed to a pure cubic PbS structure which are in good agreement with the literature values (JCPDS Card Number 78-1901). The broadening of the peaks indicates that the crystallite size is small. The average crystallite size of the product is calculated to be ca. 11 nm according to the Debye-Scherrer equation.<sup>16</sup>

As the morphology of particles plays an important role in generating luminescence,<sup>12</sup> we synthesized the PbS nanospheres under ultrasonic irradiation, using PVP as a template reagent. PVP can be used as a stabilizing agent.<sup>17</sup>

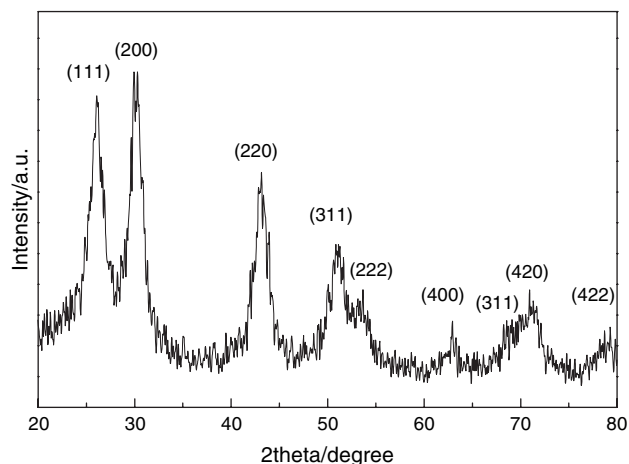


Fig. 1. XRD pattern of as-prepared products.

Also, it can control the aggregation of particles in solution, which leads to particles with similar sizes.<sup>4</sup> TEM and SEM studies show that the as-synthesized products have a uniform and regular spherical morphology with an average diameter of 110 nm (Fig. 2). The coarse surface of these nanospheres shows that they are composed of small nanoparticles with diameter of about 10 nm, which is consistent with the XRD result.

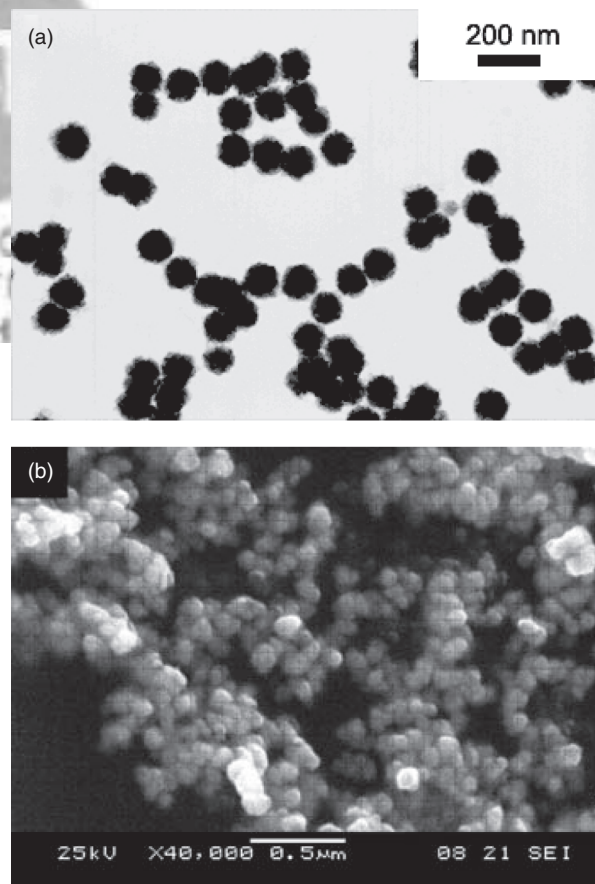
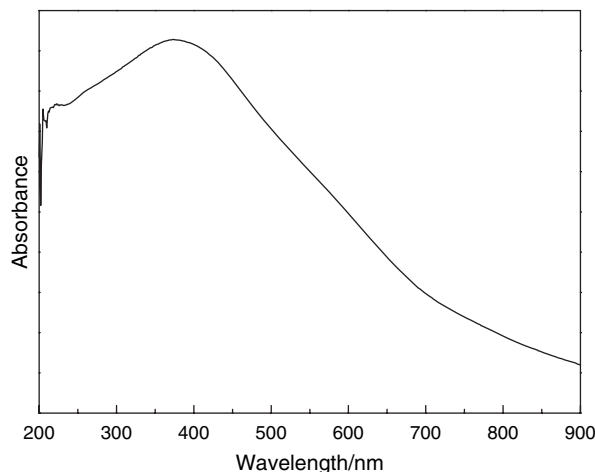


Fig. 2. (a) TEM image and (b) SEM image of the PbS nanospheres.



**Fig. 3.** The UV-Vis absorption spectrum of the PbS nanospheres.

The UV-vis absorption spectrum of the PbS nanoassemblies was measured, as shown in Figure 3. It can be seen that the absorption peak of PbS colloidal solution occurred at 374 nm, with a calculated band gap of 1.89 eV (Fig. 4), which is larger than the reported value of bulk PbS ( $E_g = 1.74$  eV). This band gap value can be attributed to the small size of PbS quantum dots of which the spheres are made up.

### 3.2. Possible Sonochemical Formation Mechanism

In recent years, ultrasound has become an important tool in chemistry for its applications in the synthesis and modification of both organic and inorganic materials.<sup>18</sup> When liquids are irradiated with high-intensity ultrasound, acoustic cavitations (the formation, growth, and implosive collapse of the bubbles) provide the primary mechanism for sonochemical effects, during which very high temperatures (>5000 K), pressures (>20 MPa) and cooling rates (>10<sup>10</sup> K/s) can be achieved upon the collapse of the bubbles.<sup>19</sup> An ultrasound wave that is intense enough to

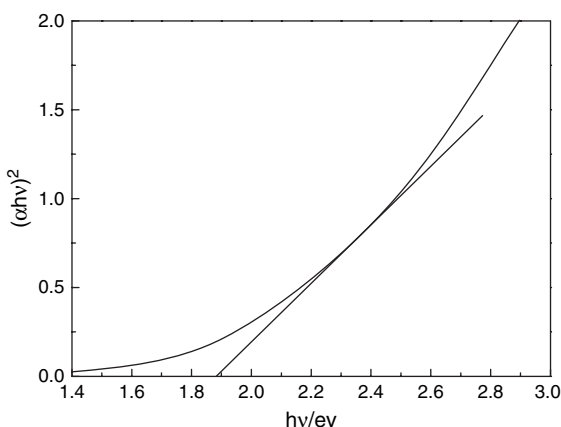
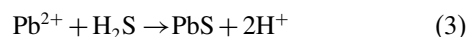


**Fig. 4.** Plots of  $(\alpha E_{\text{phot}})^2$  versus  $E_{\text{phot}}$  for band gap of the PbS nanospheres.

produce cavitation can drive chemical reactions such as oxidation, reduction, dissolution, and decomposition.<sup>20</sup>

The mechanisms for the formation of PbS nanoparticles are probably related to the radical species generated from water molecules by the absorption of the ultrasound energy. It has been known that during an aqueous sonochemical process, the elevated temperatures and pressures inside the collapsing bubbles cause water to vaporize and further pyrolyze into H· and OH· radicals. The probable reaction process for the sonochemical formation of PbS nanoparticles in aqueous solution can be summarized as follows:



Reaction (1) represents the formation of primary radicals by the ultrasound-initiated dissociation of water within the collapsing gas bubbles. Reactions (2–3) represent the main steps leading to the formation of PbS nanoparticles. The H· is a highly reducing radical, and can react with TAA rapidly via reaction (2) to form H<sub>2</sub>S. Then H<sub>2</sub>S combine with Pb<sup>2+</sup> via reaction (3) to yield PbS nuclei. These freshly formed nuclei in the solution are unstable and have the ability to grow into larger PbS particles and become stable finally.

### 3.3. Electrogenerated Chemiluminescence

Figure 5 shows the ECL-potential and CV curves of the as-prepared PbS assemblies in 0.1 M K<sub>2</sub>S<sub>2</sub>O<sub>8</sub> + 0.1 M KOH aqueous solution containing 0.1 M KCl as the supporting electrolyte. The potential sweeps were started at 1.0 V and initially went to the cathodic direction. Light

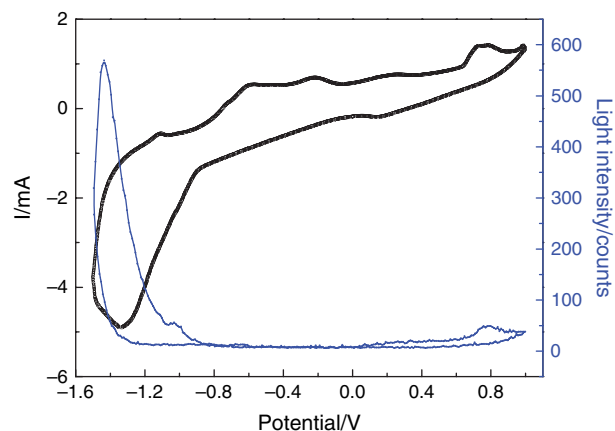
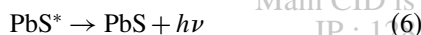


**Fig. 5.** Cyclic voltammograms and ECL curves of the PbS nanospheres in 0.1 M K<sub>2</sub>S<sub>2</sub>O<sub>8</sub> + 0.1 M KCl + 0.1 M KOH aqueous solution at a scan rate of 100 mV/s.

emission was observed when the electrode potential was cycled between  $-1.5$  V and  $+1.0$  V at a scan rate of  $100$  mV/s. Strong ECL signal is detected around  $-1.4$  V.

As shown in Figure 5, reduction and oxidation peaks appear at  $-1.35$  V and  $+0.78$  V, respectively, which can be correlated to the electron transfer at LUMO and HOMO. It is in good agreement with the light emission peak potential of PbS nanospheres. The electron band gap between these two peaks is  $2.11$  eV, a value comparable to the  $1.89$  eV obtained spectroscopically. Two voltammetric waves can be found at  $-1.1$  V and  $-0.65$  V, which can be explained by the cathodic reduction reactions of the PbS nanospheres.<sup>21</sup>

Electrogenerated reduced species ( $\text{PbS}^{\cdot-}$ ) can collide with the oxidized species ( $\text{PbS}^{\cdot+}$ ) in an annihilation process to produce excited species ( $\text{PbS}^*$ ), which generated the luminescence.<sup>11</sup> According to this annihilation theory, a proposed mechanism was suggested as follows:



However, in the presented experiments, much higher ECL can be observed when persulfate was introduced into the solution. When the potential applied to the negative direction,  $\text{S}_2\text{O}_8^{2-}$  ion was reduced to a strong oxidant  $\text{SO}_4^{\cdot-}$ .<sup>10</sup> It means that oxidized forms of PbS are not stable enough to react with the reduced forms and generate luminescence. Persulfate was a proper coreactant in this system. In other words, electrogenerated reduced forms produced in the negative potential region are stable enough to maintain their states until they react with  $\text{SO}_4^{\cdot-}$ . The formed sulfate radicals ( $\text{SO}_4^{\cdot-}$ ) can inject a hole of PbS. The intermediate can react with the negatively charged PbS nanospheres by injecting a hole into the valance band of PbS, which generated the excited  $\text{PbS}^*$  and light emission.

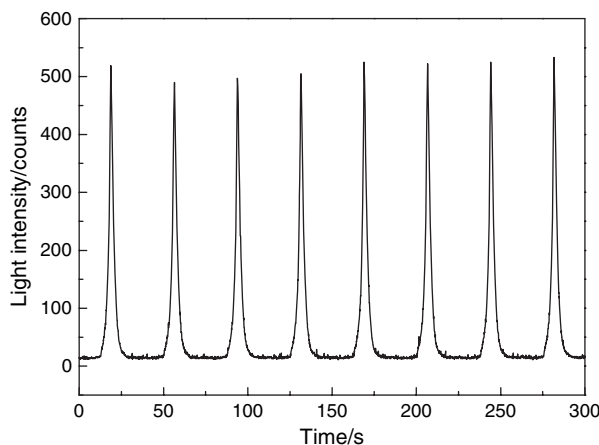
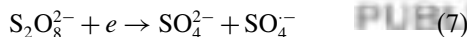
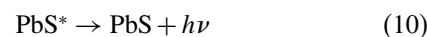
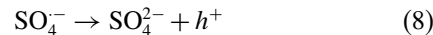


**Fig. 6.** ECL emission from PbS nanospheres in  $0.1$  M  $\text{K}_2\text{S}_2\text{O}_8 + 0.1$  M  $\text{KCl} + 0.1$  M  $\text{KOH}$  aqueous solution under continuous cyclic voltammetry for seven cycles.



We also studied the stability of luminescence. Figure 6 shows the ECL emission of PbS nanospheres under continuous potential scanning for seven cycles. The light emission shows quite good stability. This can be attributed to the aggregation morphology of the PbS nanospheres and the addition of the coreactant.

## 4. CONCLUSION

In summary, the PbS nanospheres were successfully prepared by using PVP as a template agent under ultrasonic irradiation. The formation mechanism is related with the sonochemical effect. The ECL emission of PbS nanospheres in alkali solution was first observed during potential cycling between  $+1.0$  V and  $-1.5$  V. An efficient injection of a hole into the PbS nanospheres from coreactant  $\text{K}_2\text{S}_2\text{O}_8$  can produce a higher ECL emission. Stable emission could be beneficial to find use of PbS in luminescence devices.

**Acknowledgments:** We thank the National Natural Science Foundation of China for financial support of this research (20635020, 90606016, 20575026). This work is also supported by the Jiangsu Scientific Foundation of China (BK2006114).

## References and Notes

1. V. L. Colvin, M. C. Schlamp, and A. P. Alivisatos, *Nature* **370**, 354 (1994).
2. D. L. Klein, R. Roth, A. K. L. Lim, A. P. Alivisatos, and P. L. McEuen, *Nature* **389**, 699 (1997).
3. B. A. Ridley, B. Nivi, and J. M. Jacobson, *Science* **286**, 746 (1999).
4. A. A. Patel, F. X. Wu, J. Z. Zhang, C. L. Torres-Martinez, R. K. Mehra, Y. Yang, and S. H. Risbud, *J. Phys. Chem. B* **104**, 11598 (2000).
5. S. Gallardo, M. Gutierrez, A. Henglein, and E. Janata, *Ber Bunsenges. Phys. Chem.* **93**, 1080 (1989).
6. T. Ding and J. J. Zhu, *Mater. Sci. Engin. B* **100**, 307 (2003).
7. L. Qi, Y. H. Ni, Y. Gui, J. M. Hong, and X. Zheng, *Mater. Chem. Phys.* **89**, 379 (2005).
8. M. Ichimura, T. Narita, and K. Masui, *Mater. Sci. Engin. B* **96**, 296 (2002).
9. Y. J. Yang, L. Y. He, and Q. F. Zhang, *Electrochem. Commun.* **7**, 361 (2005).
10. Z. Ding, B. M. Quinn, S. K. Haram, L. E. Pell, B. A. Korgel, and A. J. Bard, *Science* **296**, 1293 (2002).
11. N. Myung, X. Lu, K. P. Johnston, and A. J. Bard, *Nano Lett.* **4**, 183 (2004).
12. T. Ren, J. Z. Xu, Y. F. Tu, S. Xu, and J. J. Zhu, *Electrochem. Commun.* **7**, 5 (2005).
13. N. Myung, Z. Ding, and A. J. Bard, *Nano Lett.* **2**, 1315 (2002).
14. Y. Bae, N. Myung, and A. J. Bard, *Nano Lett.* **4**, 1153 (2004).
15. J. Geng, B. Liu, L. Xu, F. N. Hu, and J. J. Zhu, *Langmuir* **23**, 10286 (2007).

16. H. Klug and L. Alexander, *X-ray Diffraction Procedures*, Wiley, New York (1962), p. 125.
17. I. Pastoriza-Santos and L. M. Liz-Marzán, *Langmuir* 18, 2888 (2002).
18. (a) M. M. Mdleleni, T. Hyeon, and K. S. Suslick, *J. Am. Chem. Soc.* 120, 6189 (1998); (b) A. Gedanken, *Ultrason. Sonochem.* 11, 47 (2004).
19. K. S. Suslick, S. B. Choe, A. A. Cichowlas, and M. W. Grinstaff, *Nature* 353, 414 (1991).
20. (a) K. S. Suslick, *Ultrasound: Its Chemical, Physical and Biological Effects*, VCH, Weinheim, Germany (1988); (b) K. S. Suslick, D. A. Hammerton, and R. E. Cline, *J. Am. Chem. Soc.* 108, 5641 (1986).
21. S. W. Chen, L. A. Truax, and J. M. Sommers, *Chem. Mater.* 12, 3864 (2000).

Received: 5 February 2008. Accepted: 10 July 2008.

Delivered by Ingenta to:  
Main CID is 80004805 (JPP)  
IP : 128.135.12.127  
Tue, 09 Jun 2009 02:31:19

